Int. J. Heat Mass Transfer. Vol. 26, No. 1, pp. 11–21, 1983
Printed in Great Britain

0017-9310/83/010011-11 $03.00/0

HEAT CONDUCTION IN ECCENTRIC ANNULI

Y. P. TING* and K. L. PEDDICORD
Department of Nuclear Engineering, Oregon State University, Corvallis, OR 97331, U.S.A.

(*Received* 24 *April* 1981 *and in final form* 3 *May* 1982)

Abstract—Under the assumption of constant properties and negligible axial effects, heat conduction in the radial direction through concentric annuli is a straightforward, 1-dim. problem. However, when the annular region is shifted from the centerline, the analysis must be made in two dimensions. A theoretical, experimental, and numerical study has been made of the 2-dim. temperature distributions for a system of eccentric annuli. Two boundary conditions are examined. The first is an angular temperature function on the outer boundary. The second is a convective boundary condition with a constant heat transfer coefficient and a constant ambient temperature. The general solutions are described which are valid for any size annular region and any degree of eccentricity. The evaluation of the analytical solutions are verified by an appropriate experiment. Several numerical approximations are examined for their suitability in handling the eccentric problem.

NOMENCLATURE

c, thickness of the outer tube;
$C_n^{(1)}, C_n^{(2)}, C_n^{(3)}, C_n^{(4)}, C_n^{(5)}$, arbitrary constants of the temperature solutions;
d, eccentric displacement;
$\hat{\mathbf{e}}_\rho, \hat{\mathbf{e}}_r, \hat{\mathbf{e}}_\phi, \hat{\mathbf{e}}_\theta, \hat{\mathbf{e}}_x, \hat{\mathbf{e}}_y$, unit vectors in their respective directions;
$G(\phi)$, width of the intermediate annular region as a function of angle;
h, heat transfer coefficient;
$k_2(\phi)$, angular dependent thermal conductivity in the intermediate annular region;
k_i, thermal conductivity in region i;
M, number of terms used in the fitted temperature function, $T_0(\phi)$;
N, number of temperature solution terms used in the analysis;
$\hat{\mathbf{n}}$, unit vector normal to the outer tube inner face boundary;
q_i, volumetric heat source density in region i;
$\mathbf{q}_i(r, \theta), \mathbf{q}_i(\rho, \phi)$, heat flux vectors in region i with their respective coordinate systems;
ΔR, width of the intermediate annular region for concentric case (constant);
R_1, radius of the heater rod;
R_2, R_3, outer tube inner and outer radius;
r, radial variable in (r, θ) coordinate;
T_{bulk}, ambient temperature of the pipe system;
$T_i(r, \theta), T_i(\rho, \phi)$, temperature profile in region i with their respective coordinate system;
$T_0(\phi)$, temperature distribution on the outer tube surface;
ΔT, temperature difference across the intermediate annular region.

Greek symbols

ϕ, azimuthal variable in (ρ, ϕ) coordinate system;
θ, azimuthal variable in (r, θ) coordinate system;
ρ, radial variable in (ρ, ϕ) coordinate system.

1. INTRODUCTION

MULTI-REGION annular geometry is a basic feature of energy systems ranging from heat exchangers to fission reactor fuel elements. For the symmetric case, heat conduction through annular regions is well defined. However, if one of the internal regions is displaced radially, analysis of the system must be made in two dimensions. The purpose of this study is to determine, within the context of the specified assumptions, the theoretical solutions for heat conduction in eccentric annuli, to verify the solutions with an appropriate experiment, and to assess various numerical algorithms for calculating the temperature field within the system. The analytical solution further serves as a benchmark against which numerical approximations for treating the eccentric problem can be evaluated.

In this paper, Section 2 presents the theoretical study of heat conduction in eccentric annuli, including the procedure to determine the arbitrary constants of the solution. Section 3 covers the experimental study and the verification of the computational results from the analytical solution. In Section 4, a summary is given of the capability of several numerical approaches to effectively calculate the temperature fields for the eccentric situation.

2. THEORETICAL STUDY

A system of eccentric annuli is shown in Fig. 1 consisting of an inner cylinder, an intermediate annular region, and an outer tube. The cylinder is shifted with respect to the outer tube such that the origins of

* Present address: Southern California Edison Company, P.O. Box 800, 2244 Walnut Grove Avenue, Rosemead, CA 91770, U.S.A.

the coordinate systems for the various regions are separated by a distance d. In the theoretical study, the width of the intermediate annular region is not restricted.

2.1. *General considerations and solutions*

In defining the eccentricity problem as shown in Fig. 1, the dominant characteristic is the mixing of coordinate systems. For the asymmetric case, the polar coordinate system (r, θ) describing the cylinder is distinct from the (ρ, ϕ) system used for the outer tube, as shown in Fig. 2. Positions in the intermediate annular region may be described by either coordinate system. When the intermediate annular region is a narrow gas gap, the distinction between the two coordinate systems becomes small and may be ignored. Even if bipolar systems are used, it is still necessary to retain two coordinate systems to describe the problem.

The following options are used:

(1) Thermal conductivity is constant in each region.
(2) The volumetric heat generation rate is uniform across the inner cylinder or heater rod. No heat is generated in the other two regions.
(3) Axial effects are negligible.
(4) Steady state is assumed.
(5) The boundary condition on the outer surface of the outer tube is specified.
(6) The eccentric displacement is known.

The governing equation in each region has the form

$$\frac{1}{r}\frac{\partial}{\partial r}\left(r\frac{\partial}{\partial r}T_i(r,\theta)\right)+\frac{1}{r^2}\frac{\partial^2}{\partial\theta^2}T_i(r,\theta)+\frac{q_i}{k_i}=0 \quad (1)$$

where the subscript $i = 1$ indicates the central rod, $i = 2$ denotes the intermediate annular region and $i = 3$ represents the outer tube. The other symbols assume their usual meaning as specified in the Nomenclature. The volumetric heat source density, q_i, is only non-zero in the central or heater rod region ($i = 1$). The (r, θ) coordinate system is used for both the central and intermediate annular regions. For the outer tube ($i = 3$), equation (1) is rewritten in the (ρ, θ) coordinate system.

Solutions to the governing differential equations can be obtained directly for each of the regions. In the central region, for bonded temperatures, the equation is

$$T_1(r,\theta)=C_0^{(1)}-\frac{q_1 r^2}{4k_1}+\sum_{n=1}^{\infty}C_n^{(1)}r^n\cos(n\theta). \quad (2)$$

For no heat source, the solution of Laplace's equation in the intermediate annular region is

$$T_2(r,\theta)=C_0^{(2)}+C_0^{(3)}\ln r+\sum_{n=1}^{\infty}(C_n^{(2)}r^n+C_n^{(3)}r^{-n})\cos(n\theta). \quad (3)$$

For the outer tube, which is described by the (ρ, ϕ) coordinate system, the solution is

$$T_3(\rho,\phi)=C_0^{(4)}+C_0^{(5)}\ln\rho+\sum_{n=1}^{\infty}(C_n^{(4)}\rho^n+C_n^{(5)}\rho^{-n})\cos(n\phi). \quad (4)$$

In each solution, the arbitrary constants, indicated by C_n, superscripted 1–5 ($n \geq 0$), must be determined from the continuity and boundary conditions.

2.2. *Boundary and continuity conditions*

To obtain the complete solutions for the temperature field in each region, the usual conditions of continuity of temperature and heat flux at each interface are imposed. This is quite straightforward at $r = R_1$ in Fig. 2. However, at the interface between the intermediate annular region and the outer tube, $\rho =$

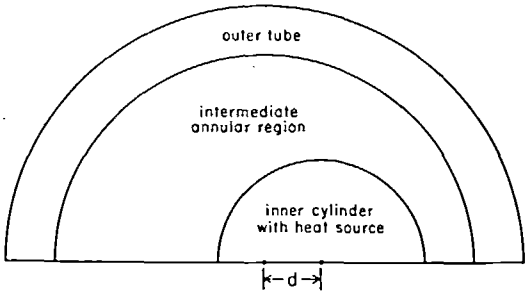

FIG. 1. Eccentric annuli.

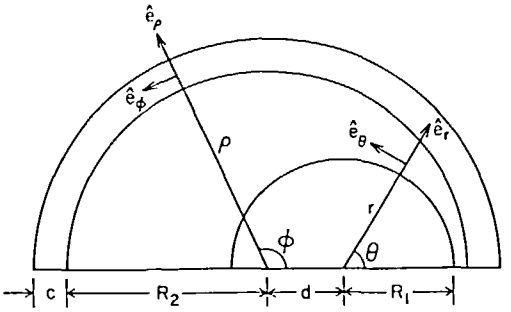

FIG. 2. Polar coordinate system for various regions.

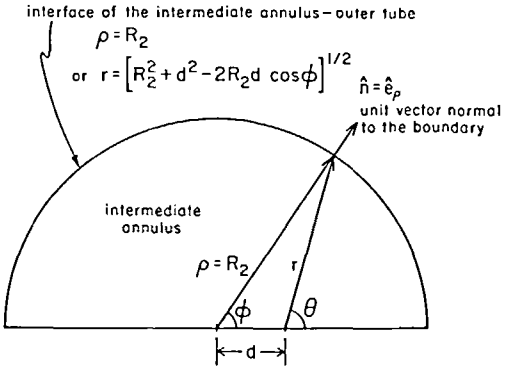

FIG. 3. Description of the boundary between the annulus and the outer tube boundary.

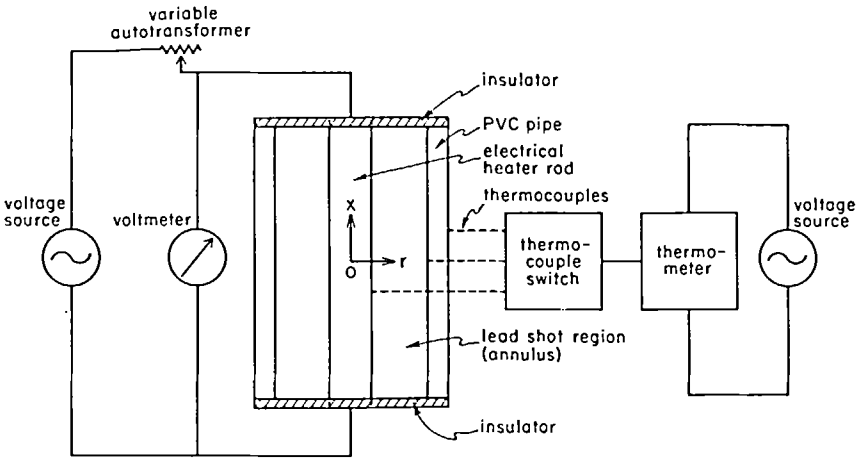

FIG. 4. Schematic diagram of the experimental apparatus.

R_2, the heat flux continuity condition must be examined in greater detail. To satisfy the heat flux condition, the components of the heat flux vectors normal to the interface must be continuous. This can be written as

$$\hat{\mathbf{n}} \cdot \mathbf{q}_2(r, \theta)\big|_{\rho = R_2} = \hat{\mathbf{n}} \cdot \mathbf{q}_3(\rho, \phi)\big|_{\rho = R_2} \tag{5}$$

where $\hat{\mathbf{n}}$ is the unit vector normal to the interface $\rho = R_2$. On the outer boundary of the system, $\rho = R_2 + c$, one of two conditions are imposed: either a specified distribution for the temperature on the surface, $T_0(\phi)$, or a convective boundary condition with a given heat transfer coefficient, h, and bulk fluid temperature, T_{bulk}, both taken to be constant.

To utilize the continuity condition specified by equation (5), the $\rho = R_2$ boundary must be related to the (r, θ) coordinate system and the displacement, d. As shown in Fig. 3, the following relationships hold at $\rho = R_2$;

$$r = r_b(d, \phi) = (R_2^2 + d^2 - 2R_2 d\cos\phi)^{1/2}, \tag{6a}$$

$$\theta = \theta_b(d, \phi) = \tan^{-1}\left[\frac{\sin\phi}{\cos\phi - (d/R_2)}\right]. \tag{6b}$$

The unit vector normal to the interface is given simply by $\hat{\mathbf{e}}_\rho$. When the definitions of the heat flux vectors in the intermediate annular region and the outer tube are inserted, equation (5) becomes

$$-k_2\hat{\mathbf{e}}_\rho\left[\hat{\mathbf{e}}_r\frac{\partial}{\partial r}T_2(r, \theta) + \hat{\mathbf{e}}_\theta\frac{1}{r}\frac{\partial}{\partial\theta}T_2(r, \theta)\right]\Bigg|_{\rho = R_2} = -k_3\frac{\partial}{\partial\rho}T_3(\rho, \phi)\big|_{\rho = R_2} \tag{7}$$

To perform the dot products in equation (7), the unit vectors of the two coordinate systems are expressed in terms of a common (x, y) system as

$$\begin{aligned}
\hat{\mathbf{e}}_\rho &= \hat{\mathbf{e}}_x\cos\phi + \hat{\mathbf{e}}_y\sin\phi,\\
\hat{\mathbf{e}}_\phi &= -\hat{\mathbf{e}}_x\sin\phi + \hat{\mathbf{e}}_y\cos\phi,\\
\hat{\mathbf{e}}_r &= \hat{\mathbf{e}}_x\cos\theta + \mathbf{e}_y\sin\theta,\\
\hat{\mathbf{e}}_\theta &= -\hat{\mathbf{e}}_x\sin\theta + \hat{\mathbf{e}}_y\cos\theta.
\end{aligned} \tag{8}$$

Finally, the solutions for temperature in the intermediate annular region, equation (3), and the outer tube, equation (4), are inserted into equation (7) and the indicated derivatives performed. Trigonometric

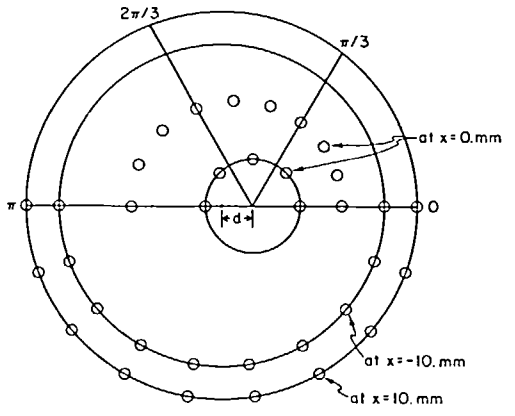

FIG. 5(a). Thermocouple locations near the axial midplane for the eccentric test with d = 10 mm.

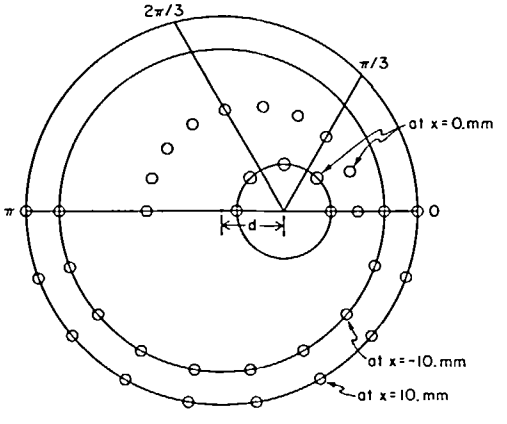

FIG. 5(b). Thermocouple locations near the axial midplane for the eccentric test with d = 20 mm.

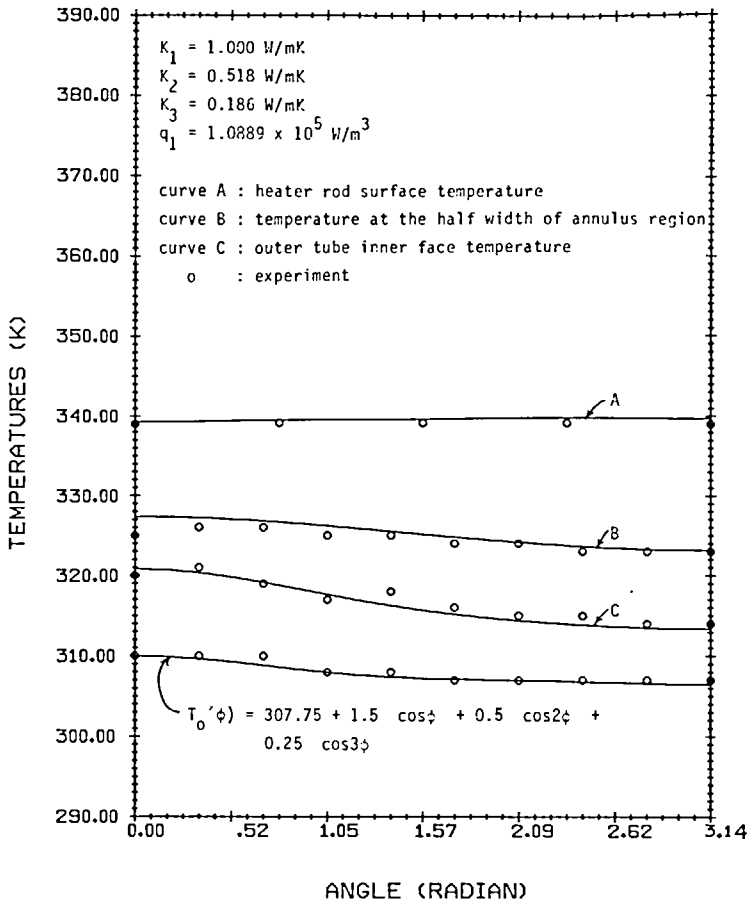

FIG. 6. Comparison of the measured and calculated temperature profiles, d = 10 mm.

relationships can be used to simplify the result such that equation (7) becomes

$$k_2\left[\cos(\phi - 0)\frac{\partial}{\partial r}T_2(r, 0) + \sin(\phi - 0)\frac{1}{r}\frac{\partial}{\partial 0}T_2(r, 0)\right]_{r = r_b(d,\phi)} = (R_2^2 + d^2 - 2R_2 d\cos\phi)^{1/2} \quad (9)$$

$$0 = 0_b(d, \phi) = \tan^{-1}\left[\frac{\sin\phi}{\cos\phi - (d/R_2)}\right] = k_3\frac{\partial}{\partial\rho}T_3(\rho, \phi)|_{\rho = R_2}.$$

A similar relationship results from the continuity of temperature condition at $\rho = R_2$ [1]. The RHS of equation (9) consists of a straightforward combination of cosine modes of the angle ϕ. The LHS, however, is a summation of a more involved set of linearly independent, continuous functions in the angle ϕ. To be able to compute the coefficients for the solution, the angular function for each term in the summation on the LHS is in turn represented by a Fourier expansion in terms of cos ($m\phi$) [1]. Finally, by exploiting orthogonality properties, equation (9) and the other continuity and boundary conditions can be reduced to a set of algebraic equations which can then be solved for the unknown coefficients. These coefficients are then inserted into equations (2)–(4), which can then be evaluated to determine the temperature field for the eccentric case.

A computer program was written to compute the coefficients C_n (superscripts 1–5, $n \geqslant 0$). An M-point Gauss–Legendre quadrature integration scheme [3] was used to evaluate the Fourier coefficients in the expansions for the interface conditions at $\rho = R_2$. The number of Gauss-Legendre integration base points must be greater than the number of terms in the expansion. This in turn is governed by the number of terms retained in the 'exact' solution for the temperature fields, equations (2)–(4). These equations were then used to determine the temperature distribution for various eccentric cases.

3. EXPERIMENTAL STUDY

The solutions represented by equations (2)–(4) must be truncated after some specific number of terms, $n = N$. Furthermore, the computations required to find the coefficients in the expansion of the interface continuity conditions are involved procedures. Consequently, to assess the evaluations of the theoretical solutions, an experimental study was performed.

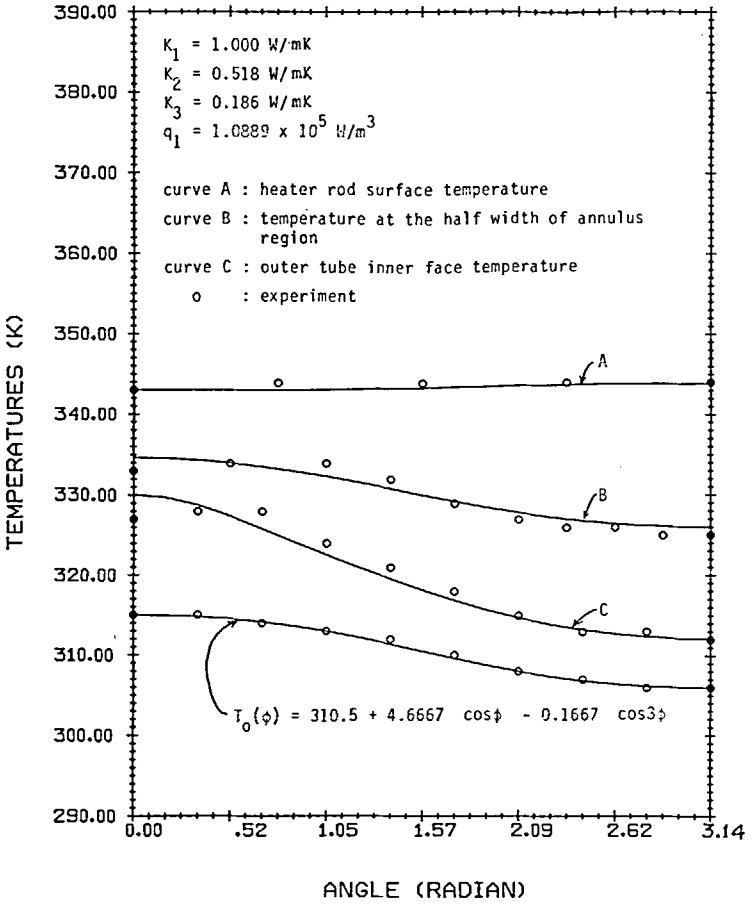

FIG. 7. Comparison of the measured and calculated temperature profiles, $d = 20$ mm.

3.1. *Experimental apparatus*

The experiment is a straightforward measurement of the 2-dim. field in an eccentric system. Particular attention was given to constructing the experiment in a manner that was consistent with the basic assumptions in the analysis.

The experimental apparatus is shown schematically in Fig. 4. The heat source was provided by an electrical heater rod, resistance 13.5 Ω, diameter of 25.27 mm, and heated length of 292.1 mm. For the outer tube, a 304.8 mm section of PVC pipe was used, inner and outer diameters of 95.6 and 114.0 mm, respectively. In the intermediate annular region, number 9 standard hard lead shot 2.2 mm in diameter, was inserted. Type J (iron vs copper–nickel alloy) thermocouples and an Omega Model 2160A digital display were used. Maximum error for the type J/2160A system is ± 1 K.

Initially measurements were made with the heater rod in the concentric position to determine the conductivity of the intermediate region containing lead shot and to evaluate the axial heat losses. The heat losses through the ends of the apparatus were found to be less than 4.3% of the power. The conductivities of the various materials showed little variation with temperature over the ranges used [1].

For the measurements, two heater rod displacements were used, $d = 10$ mm and 20 mm, where the displacement is the distance between the origin of the coordinate system for the heater rod and the origin for the outer tube. These were chosen to represent small and large degrees of eccentricity. The relative shift for the first case is 29.4%, i.e. $d/(R_2 - R_1) \times 100$ where R_1 is the radius of the heater rod and R_2 is the inner radius of the outer tube. In the second case, the relative displacement is 56.9%. More importantly, in the case of $d > R_1$, which means that the center of the outer tube no longer lies within the diameter of the heater rod [Figs. 5(a) and 5(b)]. This is a much more difficult case for several of the numerical methods to calculate, as discussed in the next section.

3.2. *Comparison of data and calculations*

Instrumentation was placed on the outer surface of the outer tube to provide the boundary temperature profile. These measurements can then be expressed in some functional form, which in turn serves as the outer boundary condition for the theoretical analysis. As mentioned in Section 2, a convective boundary condition was also studied. The heat transfer coefficient,

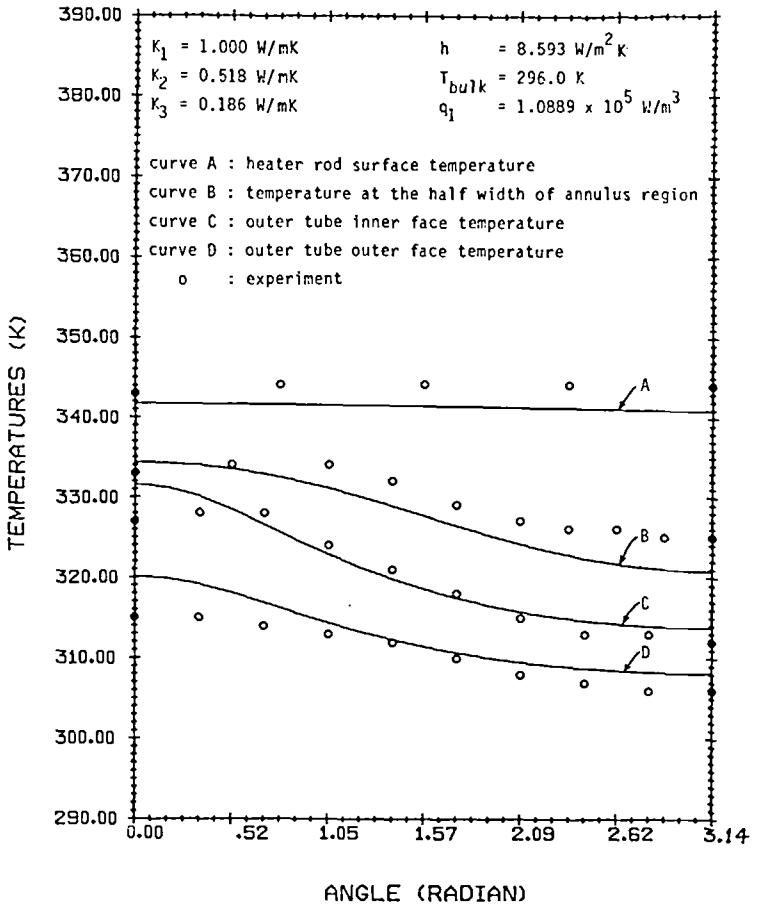

FIG. 8. Comparison of the measured and calculated temperature profiles, $d = 20$ mm, for a convective boundary condition on the outer tube surface.

determined from the concentric case, and the bulk fluid temperature were assumed to be constants.

The results are shown in Figs. 6–9. In Fig. 6, the 'small' eccentricity case ($d = 10$ mm or 29.4% eccentricity) is shown with both measured and calculated temperatures. The thermocouple positions are shown in Fig. 5(a). The function for the outer boundary temperature can be represented in the form

$$T_0(\phi) = \sum_{n=0}^{M} a_n \cos(n\phi) \qquad (10)$$

which is then used as the boundary condition for the evaluation of the theoretical solutions. The calculated and measured temperatures are within 2 K.

The case for a high degree of eccentricity is shown in Fig. 7. Here the displacement is $d = 20$ mm or 56.9%. For this case the locations of the various thermocouples are given in Fig. 5(b). The boundary condition is again fitted from measurements. Agreement between calculation and measured data for this case is to within 3 K. The largest differences occur in the narrowest segment of the intermediate region where the thermocouple wires and glues appear to perturb the heat flux and temperatures.

In Fig. 8, the large eccentricity case is again shown but with the analysis performed with a convective boundary condition. As mentioned above, the heat transfer coefficient and bulk temperature, determined from measurements made from the concentric case, were taken to be constants. Figure 8 shows that much greater deviations occur between calculation and measurement, indicating that it is not appropriate to assume a constant heat transfer coefficient around the periphery of the outer tube.

Finally, Fig. 9 depicts the effect of eccentricity on the heat removal from the system. This is shown as the fraction of total heat conducted out of the system as a function of angle. For the 10 mm, or small shift, approximately one-half of the total energy is transferred out from -1.31 radians to $+1.31$ radians. For a greater displacement of 20 mm, more angular peaking occurs in the heat transfer. Here one half of the energy is removed between -1.14 radians and $+1.14$ radians.

Based on the comparisons of Figs. 6 and 7, it is concluded that the coding and numerical evaluations of the theoretical solutions is correct. This computer program can then be used to assess various numerical methods. These results appear in the next section.

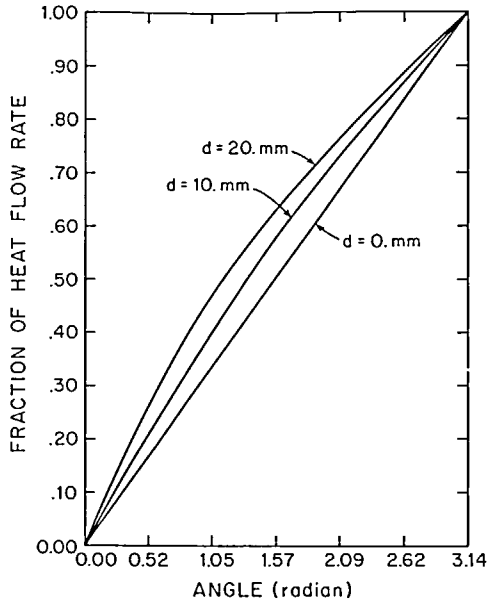

FIG. 9. The fraction of total heat conducted out of the system vs angle.

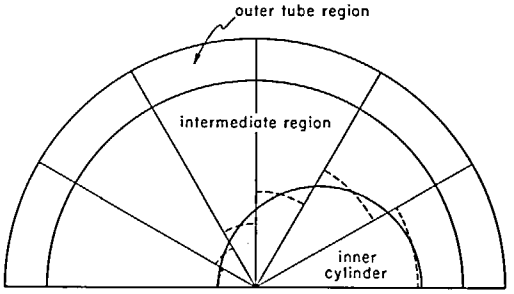

FIG. 10. Ratchet boundary approximation.

$$k_2(\phi) = k_m \cdot \frac{\Delta R}{G(\phi)}$$

$$G(\phi) = R_2 - \left[d\cdot\cos\phi + (R_1^2 - d^2\cdot\sin^2\phi)^{1/2}\right]$$

d = eccentric displacement

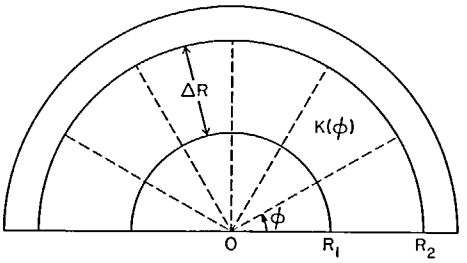

FIG. 11. Modeled conductivity approximation.

However, in practice it is recognized that the assumption of a constant heat transfer coefficient is not adequate for the analysis of the experimental apparatus.

4. NUMERICAL STUDY

For practical engineering applications, it may be necessary to determine the temperature distributions for eccentric annuli. However, the engineer wishing to analyze the problem may have neither the time nor the resources to develop and encode the solutions outlined in Section 1. In addition, some of the simplifying assumptions included in the solutions may be too restrictive. It would instead be more convenient to use one of the general purpose heat transfer programs that are readily available. The purpose of this section is to examine the capability of common numerical methods and algorithms to accurately and rapidly calculate temperature profiles in eccentric annuli. This experience may be helpful to the analyst in selecting a computational approach for a particular problem.

elements:
angular elements = 6
in heater rod region = 2
in annulus region = 3
in outer tube region = 2

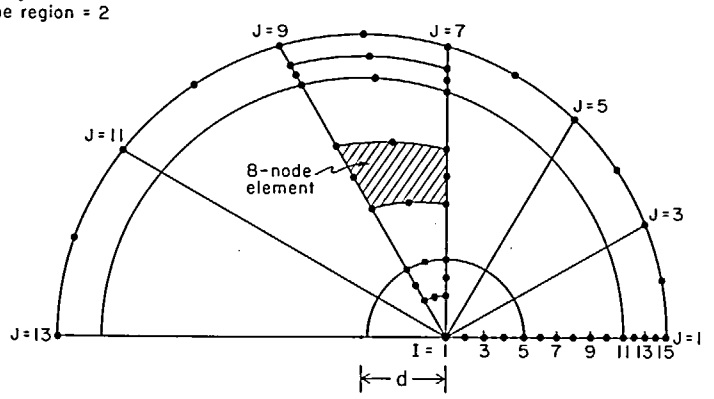

FIG. 12. Finite element model of the eccentric problem.

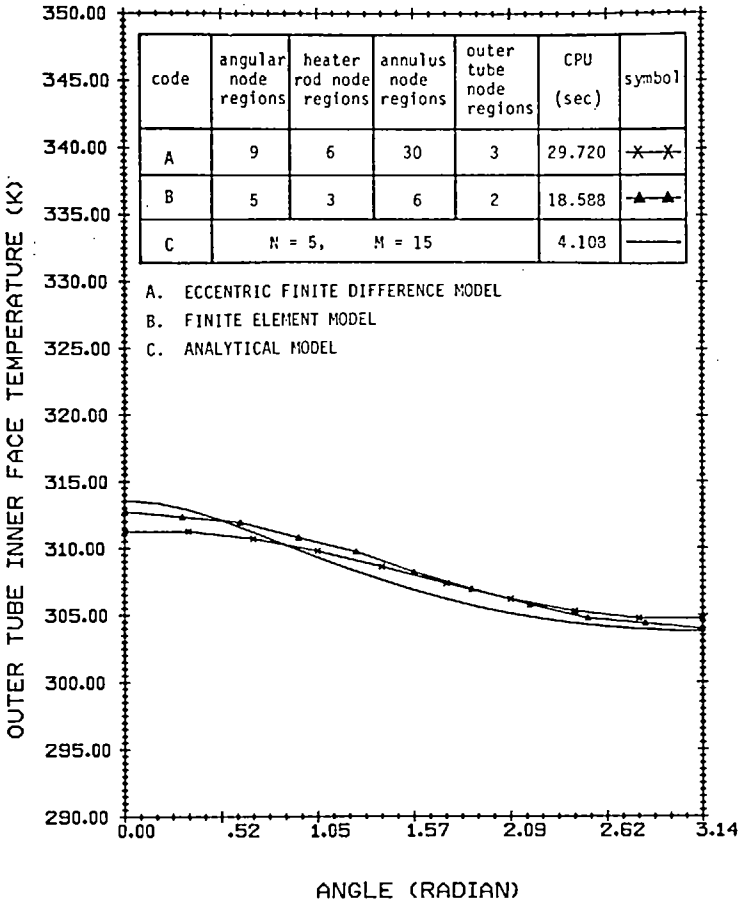

FIG. 13. Comparison of the outer tube inner face temperature for $d = 10$ mm.

Four possibilities are examined. The first two involve direct applications of the finite difference method. The third utilizes the finite element approach. The fourth is a specialized finite difference scheme developed for eccentric geometry.

4.1. *Numerical methods*

The most straightforward use of the finite difference approach to the eccentric problem is the ratchet boundary mode [1]. A single coordinate system centered within the outer tube is used. The boundary of the central tube or heater rod is approximated by a series of arcs within each angular section, as depicted in Fig. 10. This boundary then appears as a ratchet surface. The model is limited in that the eccentric displacement must be less than the radius of the inner cylinder. A second limitation of the ratchet boundary method is that, due to the geometry, a number of radial nodes equal to the number of angular regions must be used to describe the cylinder surface alone. If several angular regions are needed for the problem, the large number of nodes can lead to excessive computational time. These two limitations, however, are an inherent characteristic of the ratchet boundary model and cannot be avoided.

The second numerical approach studied is the modeled conductivity method [4]. In this case concentric geometry is retained for laying out the problem for a finite difference solution, as shown in Fig. 11. The eccentricity is accounted for by introducing an angular dependent conductivity in the intermediate region. This 'fictitious' conductivity is based on a continuity of heat flux requirement at $\rho = R$, equation (5), and has the form

$$k_2(\phi) = k_m \frac{\Delta R}{G(\phi)} \tag{11a}$$

where ΔR is the symmetric gap width and $G(\phi)$ is an angular dependent gap width determined from geometric considerations as

$$G(\phi) = R_2 - [d\cos\phi + (R_1^2 - d^2\sin^2\phi)^{1/2}]. \tag{11b}$$

In equation (11a), k_m, the actual conductivity of the material in the intermediate region, is shown as a constant but may, in fact, include temperature dependent properties and considerations for temperature jump distance or thermal accommodation coefficient for gasses as needed. This formulation of the modeled conductivity method makes it quite straightforward to easily incorporate it into a general

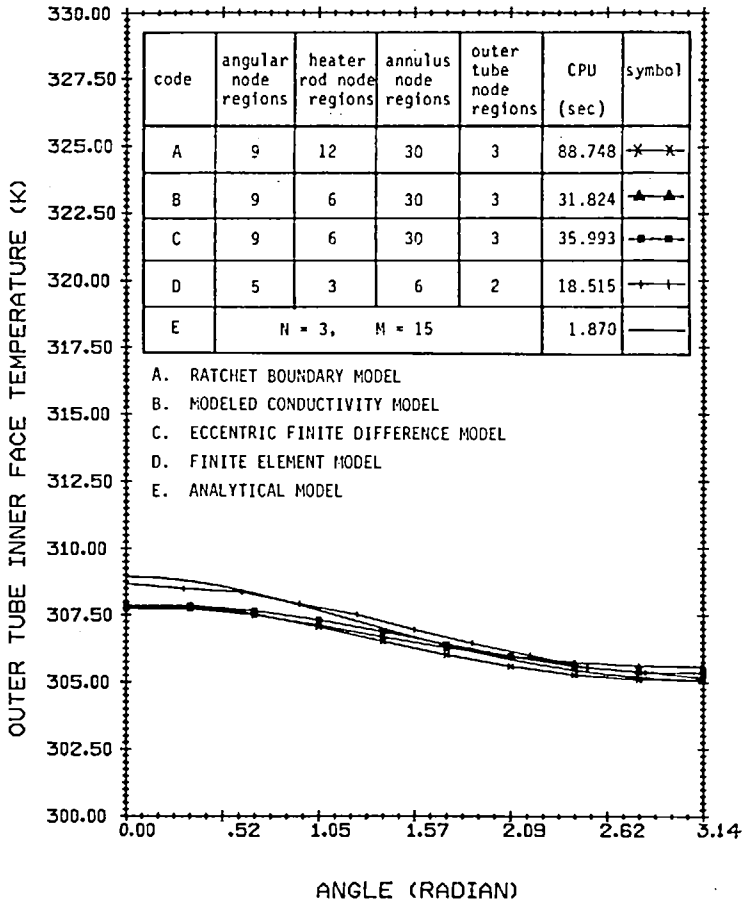

FIG. 14. Comparison of the outer tube inner face temperature for $d = 20$ mm.

purpose heat transfer code and well suited for parametric studies of eccentricity or various gap widths. Also, by using concentric geometry for the problem layout, the need for a large number of extra nodes to describe the surface of the inner cylinder is avoided. However, as can be seen by examining equation (11b), this method is restricted to displacements which are less than the radius of the inner cylinder.

The third method examined was a finite element approach. A standard heat conduction code, COYOTE, [5], was used. For the study, 8-node, quadrateral elements were used. The coordinates for the grid points of each element were obtained from straightforward geometrical relations for the eccentric problem, as shown in Fig. 12.

The main strength of the finite method is that any degree of eccentricity can be studied. However, the preparation of input is somewhat cumbersome, and it is not well suited for a large number of parametric studies.

It is possible to develop a finite difference scheme that specifically accounts for the eccentric condition. Such a scheme was derived based on equal angular regions in a 2-dim. cylindrical coordinate system with the origin located at the center of the heater rod [1]. This method is more flexible than using previously encoded general purpose finite difference programs, but requires the writing of a specialized code.

4.2. *Results and recommendations*

Several cases were used to examine the capability of the four numerical methods to calculate the temperature fields for the eccentric situation. Representative results are shown in Figs. 13 and 14. The dimensions, properties, and boundary conditions for the calculations are listed in Table 1. The comparisons are made to the analytical solution from Section 2.

From the results shown in Figs. 13 and 14, it is concluded that the finite element method produces the closest agreement with the analytical solution for both small and large degrees of eccentricity. This is not surprising since finite elements can best represent the 'off-normal' geometry posed by the eccentric problem. Due to the smaller number of elements used, a better computational efficiency is also obtained.

In cases involving smaller shifts, in which $d < R_1$, of the three finite difference approaches, the modeled conductivity method produced the best agreement with the analytical solution.

For numerical studies of an eccentric problem, it is recommended that the best and probably fastest results can be obtained with a finite element solution.

Table 1. Boundary conditions and input specifications for the numerical studies

Heater rod region	
	conductivity, $k_1 = 0.265\ W\ m^{-1}\ K^{-1}$
	radius, $R_1 = 12.635$ mm
	displacements, $d = 10.0$ and 20.0 mm
	heat source, $q_1 = 4.8423 \times 10^4\ W\ m^{-3}$
Intermediate annular region	
	conductivity, $k_2 = 0.479\ W\ m^{-1}\ K^{-1}$
	radius, $R_2 = 47.8$ mm
Outer tube region	
	conductivity, $k_3 = 0.186\ W\ m^{-1}\ K^{-1}$
	thickness, $c = 9.2$ mm
Outer boundary conditions at $\rho = R_2 + c$ (fit from measurements)	
	$T_0(\phi) = 303.0 + \cos(\phi)$ for $d = 10$ mm
	$T_0(\phi) = 303.667 + 3.0\cos(\phi) + 0.333\cos(2\phi)$ for $d = 20$ mm
Convergence criterion for finite difference calculations $= 1.0 \times 10^{-5}$	

However, for problems with small displacements, the modeled conductivity method can produce results with satisfactory accuracy but with a greatly increased flexibility which would be useful for parametric studies.

5. SUMMARY AND CONCLUSIONS

The eccentric situation can produce significant perturbations to symmetric temperature distributions, of the order of 200 K for certain situations [1, 2, 6]. The purpose of this paper was to develop and identify methods that can contribute to the solution of these problems.

In this study the analytical solutions to the governing heat conduction equations were determined for multi-region eccentric geometry. The numerical evaluation of the solutions is a somewhat tedious exercise. A computer code developed to evaluate the solutions was confirmed by experimental measurements made on a system of eccentric annuli. Of four numerical methods examined, finite elements produced the best accuracy, but the finite difference modeled conductivity approach gave satisfactory results with additional flexibility for small eccentricities. This experience may prove helpful to the analyst in selecting strategies for analyzing the eccentric problem.

Acknowledgement—The authors gratefully acknowledge the support of this research by the National Science Foundation under grant number CME-80010077.

REFERENCES

1. Y. P. Ting, Heat conduction in eccentric annuli, Ph.D. thesis, Department of Nuclear Engineering, Oregon State University (1981).
2. R. Nijsing, Temperature and heat flux distributions in nuclear fuel element rods, *Nucl. Tech.* **6**, 1–20 (1966).
3. B. Carnahan, H. A. Luther and J. O. Wilkes, *Applied Numerical Methods*. John Wiley, New York (1969).
4. G. W. McNair and K. L. Peddicord, An improved finite difference method to evaluate heat transfer in fuel pins with eccentrically placed pellets, *Nucl. Tech.* **40** (1978).
5. D. K. Gartling, COYOTE-A finite element computer program for nonlinear heat conduction problems, Sandia Laboratories, SAND77-1332 (1978).
6. G. W. McNair, K. L. Peddicord, B. D. Ganapol and R. J. Henninger, An evaluation of finite difference methods for calculating heat transfer in fuel pins with eccentrically placed pellets, *Proc. Am. Nucl. Soc. Topical Meeting on Thermal Reactor Safety*, Sun Valley, Idaho, CONF-770708 (1977).

CONDUCTION THERMIQUE DANS LES ESPACES ANNULAIRES

Résumé—Sous l'hypothèse de propriétés constantes et de conduction axiale négligeable, la conduction thermique dans la direction radiale à travers un espace annulaire est un problème simple à une dimension. Mais quand la région annulaire est déviée par rapport à la ligne des centres, l'analyse est bidimensionnelle. Une étude théorique numérique et expérimentale a été faite sur la distribution bidimensionnelle de température pour un système excentré. On examine deux conditions aux limites. La première est une fonction angulaire de température sur la frontière extérieure. La seconde est une condition de convection avec un coefficient constant de transfert thermique et une température ambiante constante. Les solutions générales sont décrites et elles sont valables pour une région annulaire de taille quelconque et un degré quelconque d'excentricité. L'évaluation des solutions analytiques sont vérifiées par une expérience appropriée. Plusieurs approximations numériques sont examinées pour leur appropriation aux problèmes d'excentration.

WÄRMELEITUNG IN EXZENTRISCHEN KREISRINGEN

Zusammenfassung—Unter der Annahme konstanter Stoffwerte und vernachlässigbarer axialer Einflüsse ist die Wärmeleitung in radialer Richtung in konzentrischen Kreisringen ein einfaches eindimensionales Problem. Wenn jedoch eine Berandung von der Mittellinie verschoben wird, muß die Berechnung zweidimensional erfolgen. Für ein System exzentrischer Kreisringgebiete wurde theoretisch, experimentell und numerisch die Temperaturverteilung bestimmt. Dabei wurden zwei Randbedingungen untersucht. Die erste ist eine winkelabhängige Temperaturfunktion für den äußeren Rand. Die zweite ist eine Randbedingung konvektiver Art mit einem konstanten Wärmeübergangskoeffizienten und einer konstanten Umgebungstemperatur. Es werden die allgemeinen Lösungen beschrieben, welche für jede Art von Ringgeometrie und jeden Exzentrizitätsgrad gelten. Die Richtigkeit der analytischen Lösungen wurde durch ein entsprechendes Experiment bestätigt. Es werden verschiedene numerische Approximationen hinsichtlich ihrer Eignung zur Behandlung des exzentrischen Problems betrachtet.

ТЕПЛОПРОВОДНОСТЬ В ЭКСЦЕНТРИЧЕСКИХ КОЛЬЦЕВЫХ КАНАЛАХ

Аннотация—В предположении постоянства свойств среды и пренебрежимо малых осевых эффектов теплопроводность в радиальном направлении в коаксиальных кольцевых каналах можно рассматривать как простую одномерную задачу. Однако в случае эксцентриситета кольцевой области должен проводиться двумерный анализ. Выполнено теоретическое, экспериментальное и численное исследование двумерных распределений температур для системы эксцентрических кольцевых каналов при двух типах граничных условий. В граничном условии первого типа задавалась температура на внешней границе как функция угла. Второй тип—это граничные условия третьего рода с постоянными коэффициентом теплоотдачи и температурой окружающей среды. Приведены общие решения, которые справедливы для кольцевой области любого размера и с любой степенью эксцентриситета. Справедливость полученных аналитических решений подтверждена соответствующими экспериментами. Предложены некоторые численные аппроксимации и проверена их пригодность для описания задачи с эксцентриситетом.